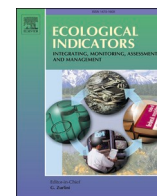


High-resolution monitoring of intra-seasonal agricultural drought using sentinel-2 and machine learning across bimodal growing seasons in Kenya

S. Mohammad Mirmazloumi, Harison Kipkulei, Rose Waswa, Tobias Landmann, Tom Dienya, Maximilian Schwarz, Fabrizio Ramoino, Clément Albergel, Gohar Ghazaryan

Angaben zur Veröffentlichung / Publication details:

Mirmazloumi, S. Mohammad, Harison Kipkulei, Rose Waswa, Tobias Landmann, Tom Dienya, Maximilian Schwarz, Fabrizio Ramoino, Clément Albergel, and Gohar Ghazaryan. 2026. "High-resolution monitoring of intra-seasonal agricultural drought using sentinel-2 and machine learning across bimodal growing seasons in Kenya." *Ecological Indicators* 185: 114790. <https://doi.org/10.1016/j.ecolind.2026.114790>.



High-resolution monitoring of intra-seasonal agricultural drought using sentinel-2 and machine learning across bimodal growing seasons in Kenya

S. Mohammad Mirmazloumi ^{a,h,*}, Harison Kipkulei ^{a,i,k}, Rose Waswa ^b, Tobias Landmann ^c, Tom Dienya ^d, Maximilian Schwarz ^e, Fabrizio Ramoino ^f, Clément Albergel ^g, Gohar Ghazaryan ^{a,j}

^a Leibniz Centre for Agricultural Landscape Research (ZALF), Germany

^b Regional Centre for Mapping of Resources for Development, Kenya

^c International Centre of Insect Physiology and Ecology, Nairobi, Kenya

^d Ministry of Agriculture and Livestock Development, Nairobi, Kenya

^e Remote Sensing Solutions GmbH, Munich, Germany

^f SERCO Italy c/o European Space Agency, Frascati, Italy

^g European Space Agency Climate Office, ECSAT, Harwell Campus, Didcot, UK

^h Technical University of Catalonia – BarcelonaTech, Spain

ⁱ Centre for Climate Resilience, University of Augsburg, Germany

^j Geography Department, Humboldt-Universität zu Berlin, Germany

^k Department of Geomatic Engineering and Geospatial Information Systems, Jomo Kenyatta University of Agriculture and Technology, Nairobi, Kenya

ARTICLE INFO

Keywords:

Agricultural drought
Sentinel-2
Crop condition monitoring
Machine learning
Kenya

ABSTRACT

Drought presents significant challenges to agriculture, threatening food security and livelihoods, across many regions. In Kenya, recurrent droughts across diverse agro-ecological zones emphasize the urgent need for reliable and scalable drought assessment methods. Although drought assessment with various datasets has been carried out for this region, many of them often use coarse or moderate resolution data. This study uses high-resolution Sentinel-2 observations and machine learning to monitor intra-seasonal crop conditions and assess drought impacts across bimodal growing seasons. Using pixel-based supervised random forest models trained with multiple vegetation indices as input, we classify croplands into drought-affected and unaffected areas. The phenology information is integrated into the framework to take into account two growing seasons. Our results from 2016 to 2022 highlight an increasing frequency in drought-affected croplands, with 2022 exhibiting widespread crop stress, especially during the long rains season. The results have strong agreement to governmental yield statistics and national and international reports as well as regional and global drought monitoring platforms. Despite uncertainties from cloud cover, land cover misclassification, and other stressors, the proposed framework provides high-resolution and operationally relevant agricultural drought monitoring approach with high resolution at national scale. Future enhancements, including radar-based data integration and real-time monitoring and prediction, can further strengthen early warning systems, supporting policymakers in developing targeted drought mitigation strategies.

1. Introduction

Drought, a prolonged period of abnormally low rainfall or water shortage, stands as one of the most significant environmental challenges facing agricultural systems globally. It significantly affects food production, ecosystem health, and overall sustainability (The Core Writing Team IPCC, 2015). According to the Intergovernmental Panel on

Climate Change (IPCC), the frequency and severity of droughts are set to increase globally due to climate change, with notable increases already observed in recent decades. Persistent droughts can alter ecosystem functions, diminishing ecological productivity and the ability of environments to support diverse life forms (Owrangi et al., 2011; IPCC. Summary for Policymakers., 2013; The Core Writing Team IPCC, 2015).

Agriculture is one of the most affected sectors by drought (FAO,

* Corresponding author at: Leibniz Centre for Agricultural Landscape Research (ZALF), Germany.

E-mail addresses: sm.mirmazloumi@zalf.de, seyedmohammad.mirmazloumi@upc.edu (S.M. Mirmazloumi).

<https://doi.org/10.1016/j.ecolind.2026.114790>

Received 22 December 2025; Received in revised form 22 February 2026; Accepted 12 March 2026

Available online 30 March 2026

1470-160X/© 2026 The Authors. Published by Elsevier Ltd. This is an open access article under the CC BY license (<http://creativecommons.org/licenses/by/4.0/>).

2023). Globally, droughts reduce cereal yields by about 9–10% on average (Lesk et al., 2016), and the sensitivity to drought is projected to increase under future climate conditions (Leng and Hall, 2019). In East Africa, countries such as Ethiopia, Somalia, and Kenya experience frequent and prolonged droughts, resulting in considerable agricultural losses and widespread water scarcity (Gebremeskel et al., 2019; Joint Research Centre, 2022). Kenya has continued to experience increased vulnerability to droughts and other extreme climate change induced/related events. Droughts have reduced in their span of occurrence from 10 to 20 years in the 20th century to 1–2 years in the present century (Rhee et al., 2010; Ghazaryan et al., 2020a; Lam et al., 2023).

Monitoring drought hazards and impact is highly critical due to the widespread effects of drought on various sectors of the agro-ecological system. In general, drought drastically influence growth, yield, and resistance to pests and disease, along with restrictions on irrigation water use (Ghazaryan et al., 2020b; Haile et al., 2020; Santini et al., 2022; Vicente-Serrano et al., 2022).

Monitoring drought effects on croplands (e.g., growth and yield) may help to alleviate the drought effects in agriculture and overcome adopted challenges to finally mitigate the impacts of agricultural drought. Considering the effects of drought on biophysical and chemical properties of soils and plants (e.g., soil moisture, organic matter content, vegetation biomass, chlorophyll content, canopy cover, and soil temperature), monitoring technologies like remote sensing can effectively develop agricultural drought mapping by filling data gaps using consistent archive of satellite images and up to daily datasets that are freely available (Anjum et al., 2011; Hazaymeh and K. Hassan, 2016; Ghazaryan et al., 2020b; Camps-Valls et al., 2025).

Earth Observation (EO) data enable effective agricultural drought monitoring by providing extensive spatial coverage and continuous data availability. Remote sensing-based drought indices can effectively capture the onset, severity, and duration of drought conditions, aiding in the assessment and response strategies (Ghazaryan et al., 2020b). In recent years, numerous studies have utilized EO data for assessing drought impacts, though only a limited number have employed high resolution EO data for monitoring purposes. The majority of research has relied on moderate resolution data, such as MODIS (Schwarz et al., 2020).

Vegetation-related drought indices, like the Vegetation Condition Index (VCI) and Vegetation Health Index (VHI) derived from the Normalized Difference Vegetation Index (NDVI), are particularly useful for agricultural drought monitoring (Rojas et al., 2011). Ghazaryan et al. (2020b) examined several MODIS-based indices for detecting drought impacts on crop production, finding that the Evaporative Stress Index (ESI) and Land Surface Temperature (LST) indicated more severe drought conditions than NDVI. Since a single factor like vegetation growth does not offer a complete view of drought conditions, new indices integrating multiple factors with traditional meteorological datasets have been developed, such as Scaled Drought Condition Index (SDCI) (Rhee et al., 2010) and Synthesized Drought Index (SDI) (Du et al., 2013).

Regional droughts have been examined using multi-source remote sensing data, with studies employing MODIS NDVI, EVI, and TRMM data through deep learning models (Shen et al., 2019), developing composite indices combining SPI and VHI (Monteleone et al., 2020), and proposing new drought indices such as Soil Moisture Drought Index (HSMIDI) (Park et al., 2017) and GBMDI (Zhang et al., 2022). Recent high-resolution monitoring efforts leverage Sentinel-2 and field survey data for local to regional drought assessment (Ghazaryan et al., 2020a; Kowalski et al., 2023). Descals et al. (2025) integrated Sentinel-2 phenology metrics with field data to successfully detect total crop losses in winter cereals, demonstrating the value of high-resolution EO data for rapid drought impact assessments.

Despite extensive research on drought monitoring, gaps persist in operationally relevant applications. Most studies rely on moderate resolution sensors such as MODIS, constraining assessments to landscape rather than field scales. Additionally, approaches that account for agro-

ecological heterogeneity through spatially stratified modeling remain limited. Finally, multi-year, high resolution drought monitoring products with integrated quality information are largely absent at national scales.

To address these limitations, this study develops a phenology-informed, high-resolution drought impact monitoring framework. By integrating vegetation indices derived from Sentinel-2 with crop-calendar information and agro-ecological zone (AEZ) stratification, we train pixel-based Random Forest classifiers to distinguish drought-affected and unaffected croplands separately for the long and short rains seasons.

The specific objectives of this work are to (i) generate national-scale seasonal crop condition maps at 20 m resolution that capture intra-seasonal drought impacts across bimodal growing seasons of Kenya, and (ii) validate the resulting drought-affected cropland patterns using independent evidence from sub-county maize yield statistics, NDMA drought reports, and hydroclimatic anomalies derived from SPEI. The proposed framework provides an operationally relevant advancement in agricultural drought monitoring by enabling scalable, field-level drought impact assessment, supporting early warning systems and targeted drought risk management interventions across Kenya.

2. Study area

The present study covers Kenya located in the East Africa region. The area of Kenya is approximately 580,367 km², with approximately 2% of its landmass covered by water. Of the total land area, 18% of the land has medium to high potential for agricultural use. Kenya is divided into seven major Agro-Ecological Zones (AEZ), which are characterized based on soil and climatic conditions (Fig. 1). The climate is moderated largely by the varying topography, and the influence of the Indian Ocean and Lake Victoria. The average temperature across the country varies between 15 °C and 35 °C within a year. Total annual precipitation ranges from 200 mm to 2200 mm. The rainfall pattern is bimodal with long rains experienced between March and June, and short rains between October and December.

Agriculture is the backbone of the economy in Kenya and relies mostly on rainfall, while irrigated agriculture constitutes only 2.4% of the cultivated land in Kenya (FAO, 2015). Subsistence crops such as maize, beans, and sorghum are grown predominantly on small farm (typically under 2 ha), largely under the smallholder farming systems. Cash crops such as tea, cotton, sugarcane, and coffee are grown on large farm sizes.

Kenya has recorded 28 major droughts in the last 100 years, with frequencies increasing in the recent decades (Huho and Mugalavai, 2010), and has experienced frequent droughts in the recent past (see Fig. 2). Notable severe droughts since the 1980s include the 1983–1984 event with up to 75% rainfall deficiency that devastated staple crop production (Shisanya, 1990), the 1999–2000 drought considered among the worst on record, and the 2004–2006 drought that affected even typically high-potential regions and pushed nearly 3 million people into food crisis (Kandji, 2006). More recent droughts in 2008–2009, 2016–2017, and 2020–2022 have continued this trend of increasing vulnerability (Muller, 2014; CDKN Global, 2017; D'Ercole et al., 2024).

To highlight the drought condition in Kenya, Fig. 2 shows the conditions in the recent years based on the time series of Standardized Precipitation-Evapotranspiration Index (SPEI) and precipitation patterns in Kenya from 2016 to 2022 using ERA5-Land monthly aggregated dataset.

3. Data

3.1. Earth observation data

Sentinel 2 data and spectral indices or vegetation indices (VIs) derived from it were selected as the main input data for crop condition

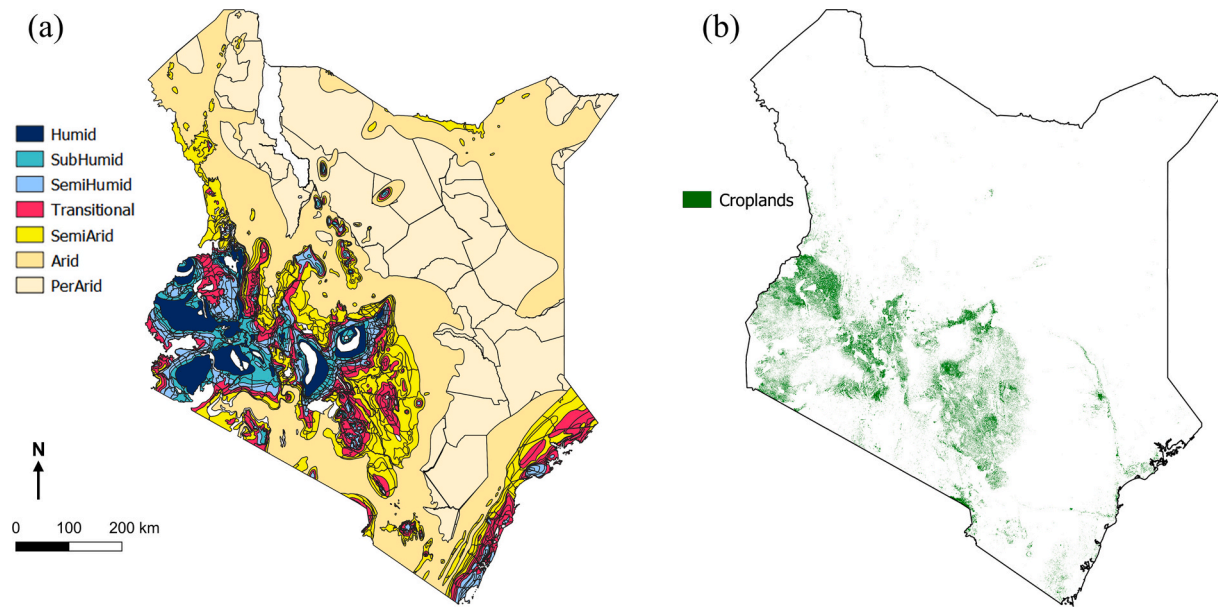


Fig. 1. Geographic representation of agricultural landscapes in Kenya. Fig. 1a the top map (a) displays the Agro-ecological zones (AEZ) of Kenya, provided by the Regional Centre for Mapping of Resources and Development (RCMRD). Fig. 1b illustrates the distribution of active cropland fields across Kenya, extracted from the high-resolution ESA WorldCover V.2 product.

assessment. Sentinel-2 data offers multispectral information at 10–60 m spatial resolution, enabling the exploitation of VIs for at least every 5 days (ESA, 2015). Sentinel-2 Level-2 A (L2A) data were used and information available in Scene Classification (SCL) band was used to mask pixels affected by clouds and cloud shadows (ESA, 2024).

3.2. Additional data

Several additional datasets were integrated into the framework. Land cover information from ESA WorldCover V.2 has been used as a mask to retain only cropland pixels. This map provides a global land cover map at 10-m spatial resolution based on Sentinel-1 and -2 data.

As the cropping systems in Kenya are characterized with a bimodal growing season pattern, information on phenology was also integrated in the framework based on datasets obtained from two sources. First, a survey-based crop growth stage information was provided by Ministry of Agriculture of Kenya. Specifically, information on long and short rains was provided based on timing of planting, vegetative-productive, ripening-harvest, and end of harvest. Secondly, the WaPOR Phenology dataset (Muller, 2014) was used to acquire the pixel-based phenology information at dekadal temporal scale (10-days period), determined by Van Hoolst et al. (2016) methodology using a three-year NDVI time series. Thus, the growing seasons of croplands have been identified based on the above-mentioned sources to two seasons: long rains season and short rains season.

The SPEI derived from ERA5-Land monthly precipitation and potential evapotranspiration was included as an additional indicator of water balance anomalies. Information from the NDMA was also incorporated for validation and interpretation, providing detailed observations on rainfall, vegetation condition, water and pasture availability, food security status and livestock impacts. Finally, maize yield data provided by the Ministry of Agriculture were used to evaluate the consistency between remote-sensing-based drought signals and observed production outcomes.

4. Methodology

Our proposed workflow for crop condition assessment is based on vegetation indices of Sentinel-2 images as input to the random forest

model for performing the binary classification for seasonal mapping of crop conditions in Kenya. The process consists of model training on AEZ and growing seasons independently due to heterogeneity across the study area. Fig. 3 illustrates the scheme of proposed methodology.

4.1. Growing season stratification and identification

Accurate distinction of the two main cropping seasons in Kenya was essential for analyzing drought impacts. Growing season boundaries were identified using phenological metrics rather than fixed calendar dates. The start, peak, and end of each season were determined from the WaPOR phenology dataset (Fig. 4) and crop growth stage information provided by Ministry of Agriculture of Kenya (Table 1).

The resulting seasonal masks allowed Sentinel-2 time series to be divided into long and short rains periods, ensuring that vegetation index anomalies were interpreted within the correct growth cycle. This stratification provided the temporal basis for training and applying the classification models separately for each season and AEZ.

4.2. Crop condition indicators and machine learning based classification

Sentinel-2 L2A (surface reflectance) images have been used to generate four VIs, including Normalized Difference Vegetation Index (NDVI), Normalized Difference Moisture Index (NDMI), Normalized Difference Red Edge (NDRE), and Green Normalized Difference Vegetation Index (GNDVI). The VIs were calculated from monthly median and maximum composites of preprocessed Sentinel-2 data. The composites were needed due to cloud cover impact on the individual observations and ensured continuous coverage of data across Kenya.

The computed growing season are the input to random forest model, for a binary classification. Two groups of time series were categorized by identifying local temporal anomalies. The filtering of time series stands for distinguishing time series that abnormally have low VIs values during the growing seasons. The occurred deviations indicate the changes compared to undistributed phenology. Consequently, two classes of labels are supervised based on drought unaffected and affected VIs time series.

Based on historical agricultural drought information, VIs time series from two years of 2018 and 2021 were selected for learning step of

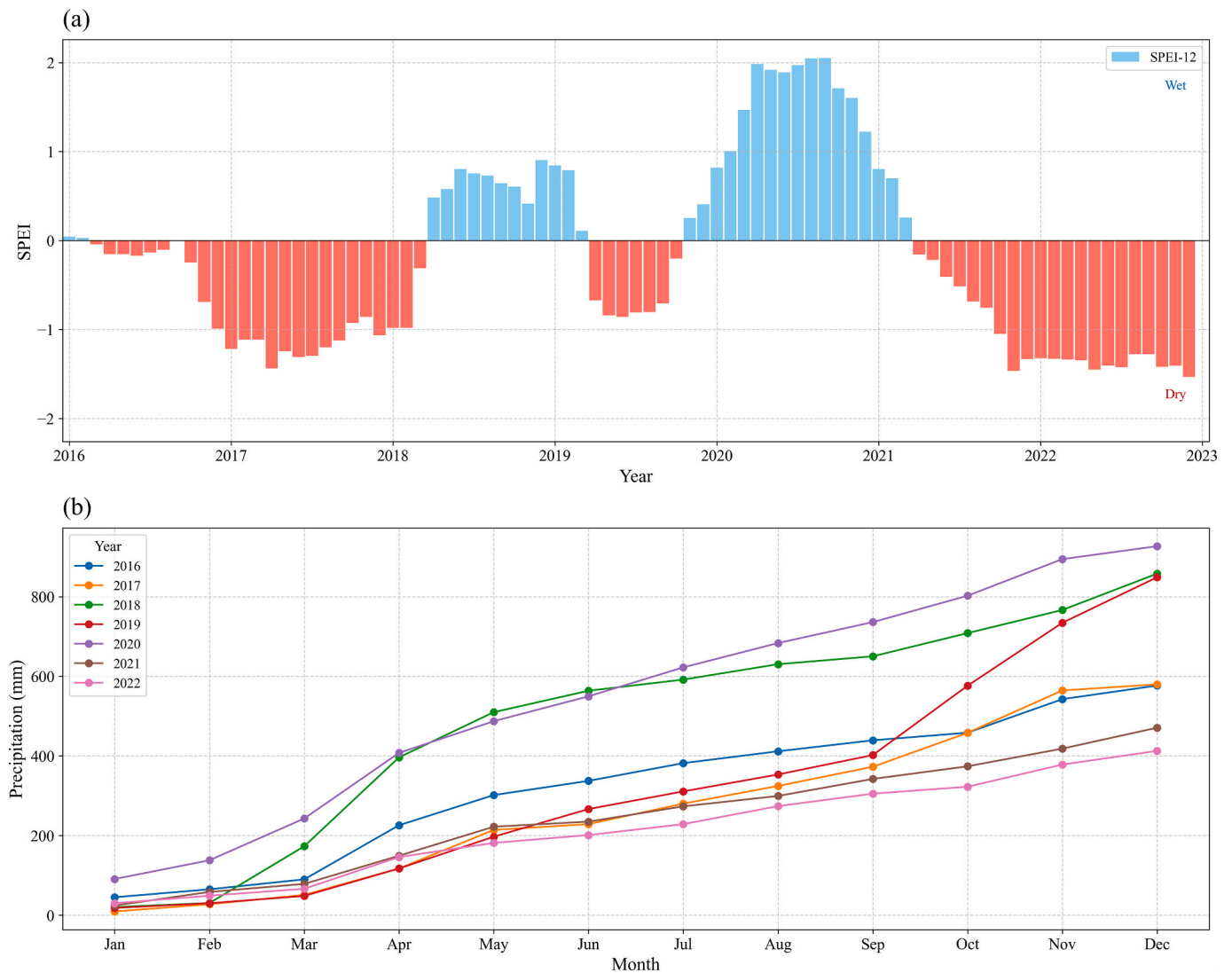


Fig. 2. Time series of drought condition and precipitation patterns in Kenya from January 2016 to December 2022. (a) The 12-month Standardized Precipitation-Evapotranspiration Index (SPEI) illustrates the severity of dry (red bars) and wet (blue bars) periods relative to the long-term average. (b) Annual cumulative precipitation curves show the progression of rainfall throughout each year, allowing for inter-annual comparison. (For interpretation of the references to colour in this figure legend, the reader is referred to the web version of this article.)

machine learning models, representing examples of non-drought and drought conditions. Based on this information, over agricultural areas labels were generated with drought and non-drought conditions. Fourteen independent models were trained per season and AEZ, one for each combination of seven AEZs and two growing seasons. AEZ-based ML model training helps mitigate the influence of administrative borders by decomposing spatial heterogeneity using relevant environmental data. This approach, increasingly adopted through AEZs and landforms, enhances the performance of ML models in heterogeneous landscapes (Khechba et al., 2024, 2025). Additionally, it provides a structured framework for balancing global and regional model performance, ensuring localized adaptability and optimizing predictive accuracy across diverse regions. For each model, the 70:30 train-test input data ratio was chosen to generate classifiers for predicting the most accurate class label (More details in Appendix). The trained models were later evaluated using the test data by confusion matrix and overall accuracy. The trained models predict crop condition maps of target years for two seasons and seven AEZ. In this work, crop condition maps of seven AEZ and two growing seasons were generated for the years 2016–2022.

4.3. Quality map

Quality maps were produced to present data reliability across different regions. The goal is to supply a visual and quantifiable representation of data reliability across different regions. To do so, a set of thresholds were established based on the probability estimations derived from random forest models predictions per pixel and corresponding number of Sentinel-2 Clear Sky Observations (CSOs). This approach can represent areas with potentially less reliable data, attributable to fewer clear observations or lower probability scores from random forest models.

The reliability of the classification was evaluated using a three-level quality map that integrates the random forest class probability with the number of valid CSOs during the growing season. Pixels with probabilities above 0.80 and more than 25 valid observations were considered high quality, those with probabilities between 0.50 and 0.80 and more than 25 valid observations were considered medium quality, and all remaining valid pixels were labeled low quality. The thresholds were empirically selected after testing different combinations to ensure spatial consistency and stable classification performance across regions with varying cloud conditions. This approach is conceptually aligned

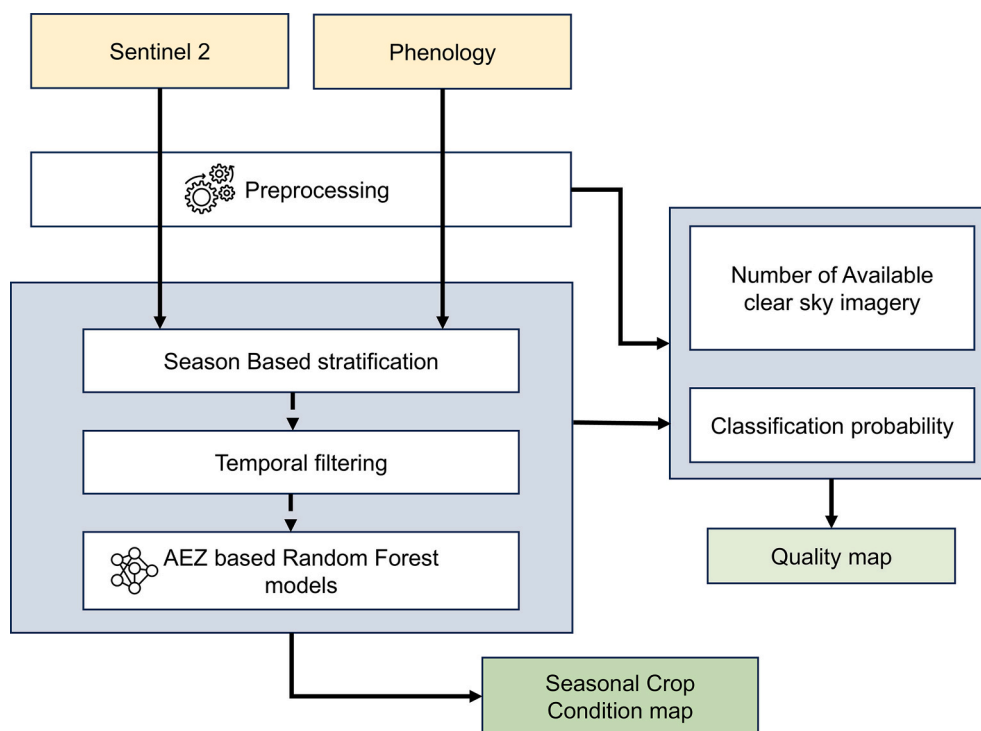


Fig. 3. Methodological workflow for generating a seasonal crop condition map and associated quality map. The process begins with the preprocessing of Sentinel-2 satellite imagery and phenology data, followed by season-based stratification and temporal filtering. AEZ based Random Forest models are then applied to produce the seasonal crop condition map.

with previous work, which emphasizes the importance of per pixel indicators of confidence or predicted accuracy (Khatami et al., 2017). While the specific implementation differs, the underlying objective of communicating spatial variation in map reliability is consistent with quality assurance and quality control recommendations (Szantoi et al., 2021; Tyukavina et al., 2025).

4.4. Validation

In addition to the performance assessment of random forest models and derivation of metrics such as overall accuracy, the outcomes of crop condition mapping have been compared to other products (indirect validation) and evaluated by users (user-based validation) (De Vos et al., 2025) to enable evaluation across broader areas and/or longer time frames. For the indirect validation scope, maize yields and NDMA reports have been utilized to relatively evaluate their discrepancies with classification outputs by intercomparison temporal and spatial consistency. Furthermore, user-based validation involves consolidating the feedback and evaluations from end-users (domestic users mainly) on the crop condition maps to identify potential discrepancies, assess the practicality of the data, and enhance its overall usefulness.

5. Results

5.1. Seasonal crop condition mapping

The crop condition outputs show the spatial characteristics of croplands affected by drought at a national scale. The maps are attributed to two supervised classes of croplands, namely unaffected pixels and drought-affected pixels. Hence, for each year, two sets of classifications were mapped, including long rains season (season 1) (Fig. 5) and short rains season (season 2) (Fig. 6). Fig. 5 shows long rains season maps indicating the effect of drought in different years. The maps show significant variation in drought conditions. In 2018 and 2020, the long rains season experienced less severe drought, with relatively fewer

cropland areas being classified as affected (indicated by red pixels). In contrast, the 2022 map shows widespread drought stress, with a substantial increase in the number of affected cropland pixels.

Fig. 7 indicates the affected area of croplands by drought over 7 years across two growing seasons. Year 2018 experienced the minimum effect of drought, particularly the long rains season, after substantial drought impacts in 2016 and 2017. Although short rains season in 2020 saw an improvement, the long rains remained more impacted, showing signs of continuing stress on crops. The sharp increase during both seasons started in 2021, and nearly 90% of croplands were affected during the long rains season of 2022. Long rains seasons showed more severe impacts than the short rains, except in 2018, followed by an increasing trend in both seasons.

The combined analysis of satellite-derived drought indicators and reported impacts highlights interannual and seasonal variability in drought impact. The proportion of croplands with drought impact was particularly high during the Long Rains seasons, which aligns with negative SPEI anomalies. The Short Rains of 2021 and 2022 also show increased areas under stress, consistent with reports of crop failure and declining livestock conditions. These outcomes demonstrate that extreme drought years are simultaneously captured in biophysical indicators and in the socioeconomic outcomes reported by national authorities.

5.2. Model performance and validation

Fig. 8 shows the performance evaluation of trained models characterized by tuned parameters over test datasets. Random Forest models achieved overall accuracies ranging from 65% to 85%, varying by season and AEZ (Fig. 8). Models for high potential agricultural zones (AEZs 1 to 3) generally showed higher accuracy than those for ASAL regions (AEZs 5 to 7), reflecting greater training sample availability and more consistent vegetation signals in higher productivity areas.

Quality maps complement crop condition outputs by indicating data reliability (Fig. 9). Central and coastal regions generally show higher

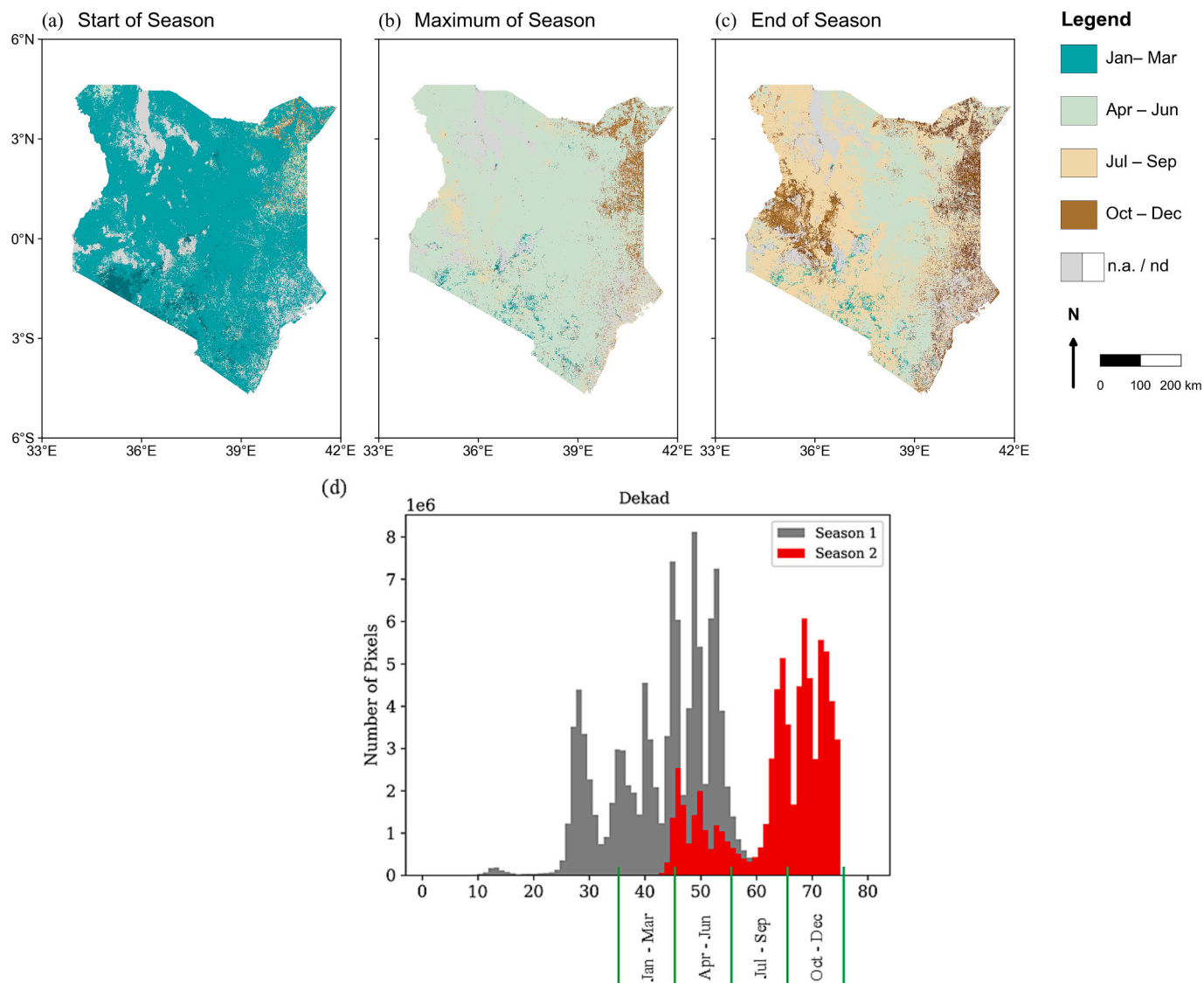


Fig. 4. WaPOR phenology (FAO, 2024) in the study area for long rain season illustrates for 2018 a) start, b) maximum and c) end of the season and d) aggregated information on both long and short rain seasons.

Table 1

Growing stages of Maize in Busia county in two seasons of long and short rains, provided by ministry of agriculture.

Season	Crop Stage	Jan.	Feb.	Mar.	Apr.	May	Jun.	Jul.	Aug.	Sep.	Oct.	Nov.	Dec.
Long Rains	Out of Season												
	Planting		█	█	█								
	Vegetative-reproductive			█	█	█	█	█					
	Ripening-harvest							█	█	█			
	End of harvest										█	█	
Short Rains	Out of Season												
	Planting							█	█	█			
	Vegetative-reproductive									█	█	█	█
	Ripening-harvest	█	█	█									
	End of harvest			█	█								

data quality, while areas with persistent cloud cover show reduced reliability. As shown in the right panel of Fig. 9, the quality map categorizes regions using a value range from 1 to 3, where 3 indicates the

highest data quality. This classification helps distinguish between areas with sufficient Sentinel-2 images and high model confidence (in green), and areas where fewer observations or lower confidence levels suggest

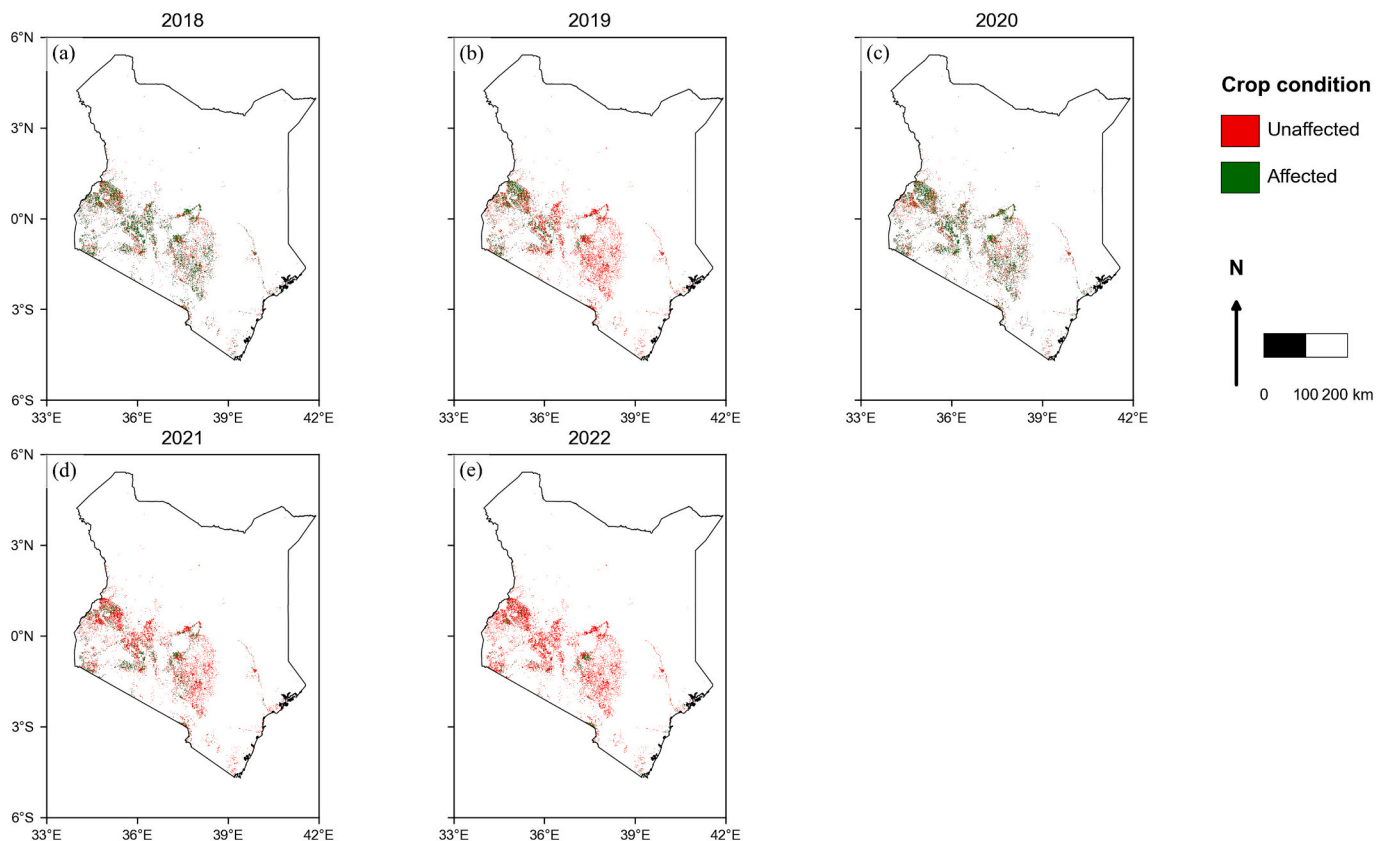


Fig. 5. Spatial distribution of crop conditions across Kenya 2018–2022 long rains seasons. The maps differentiate between unaffected croplands (green) and affected croplands (red) by drought. (For interpretation of the references to colour in this figure legend, the reader is referred to the web version of this article.)

reduced reliability (in light green and red). For instance, the central and coastal regions of Kenya have higher data quality, while the regions with yellow or grey pixels highlight areas where the results are less reliable due to factors like persistent cloud cover or lower model prediction confidence.

6. Discussion

6.1. Interannual trends and spatiotemporal patterns of drought condition

The results demonstrate that integrating high-resolution Sentinel-2 observations with phenological information enables detailed detection of drought impacts across Kenya. The derived crop condition maps reveal strong spatial and temporal variability between seasons and years, reflecting the influence of both climatic and regional factors. When compared with NDMA drought records, maize yield data, and the ERA5-Land based SPEI, the patterns of vegetation stress show consistent agreement with independently reported drought events. The NDMA reports provide qualitative and quantitative information on drought occurrences and other indicators, such as the expenditure on droughts and efforts channeled towards drought mitigation responses in various sectors. An additional advantage of the reports is that they are published annually, enabling a complete series of information for evaluating crop condition products.

The crop condition maps derived in this work reveal that 2018 was characterized by comparatively non-drought conditions, which also applied to most of the ASAL areas. However, the 2019 seasonal condition analysis revealed drought effects in most parts of the country. The assessed conditions are also in line with the NDMA reports showing widespread hydrological droughts which led to vegetation deficit in 11 ASAL counties (NDMA, 2019). The 2019 crop condition map revealed more severe drought conditions, particularly, the southeastern and

northeastern counties and the central-northern region encompassing Laikipia and Meru counties. The findings are also in line with other studies in the region that showed water scarcity situations across the country (Njogu, 2022; Lam et al., 2023).

The crop condition outcomes for 2020 revealed improved conditions relative to the 2019 period. Most of the counties in the ASAL regions recorded improved conditions. Furthermore, some counties, including Makeni, Kitui, Tana River, Meru, and Narok Counties, realized improved vegetation conditions, aligned with the NDMA report for the 2019–2020 (NDMA, 2019, 2020). The generated maps have high agreement when assessing 2022 drought, which based on classification output had the highest area affected and according to literature was the most severe in four decades, following four consecutive failed rainy seasons that resulted in cumulative rainfall (NDMA, 2019, 2020, 2021, 2022; FAO, 2024).

The 2021 crop condition products revealed that the year was marked by marginal conditions, with most counties affected, including ASAL, Nyandarua, and Nakuru counties. The poor conditions were also captured in the NDMA annual report due to the poor performance of October to December 2020 short rains and March to May 2021 long rains (NDMA, 2021). In addition, the period recorded the highest population (2.1 million people) in dire need of food assistance. The crop condition maps for 2022 indicated a continuation of the drought situation in Kitui, Makeni, Kwale, Lamu, Tana River, Kilifi, Kajiado and Narok counties, remained relatively the same in terms of drought patterns. The reports from NDMA corroborate the analyzed crop condition products, with statistics showing a worsening drought situation and an increased population of up to 3.5 million with a high level of acute food insecurity by February (NDMA, 2022).

In addition to the NDMA reports, we also utilized maize yield data provided by the Ministry of Agriculture, Livestock and Development in Kenya. Maize productivity at the sub-county level was compared with

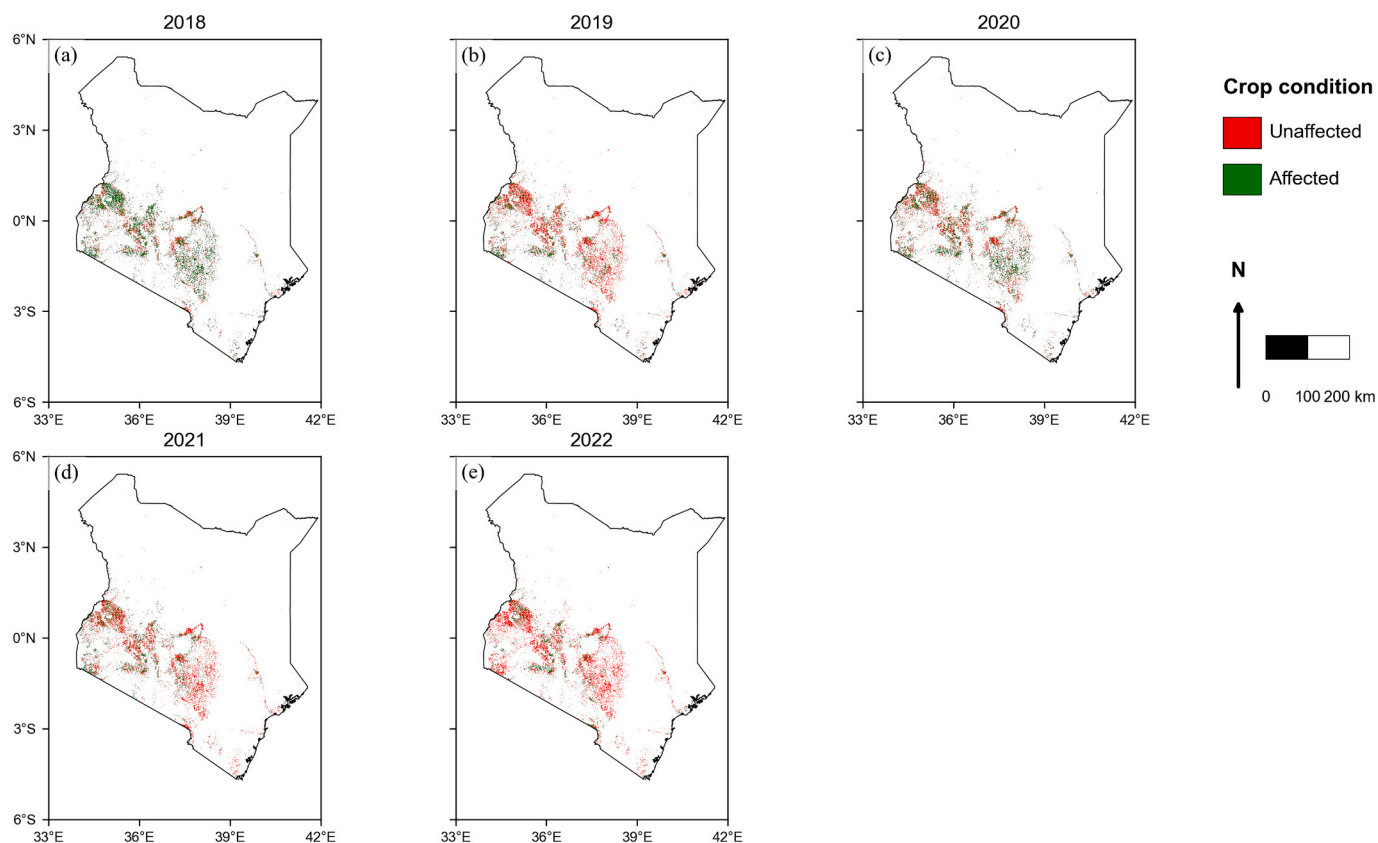


Fig. 6. Spatial distribution of crop conditions across Kenya 2018–2022 short rains seasons. The maps differentiate between unaffected croplands (green) and affected croplands (red) by drought. (For interpretation of the references to colour in this figure legend, the reader is referred to the web version of this article.)

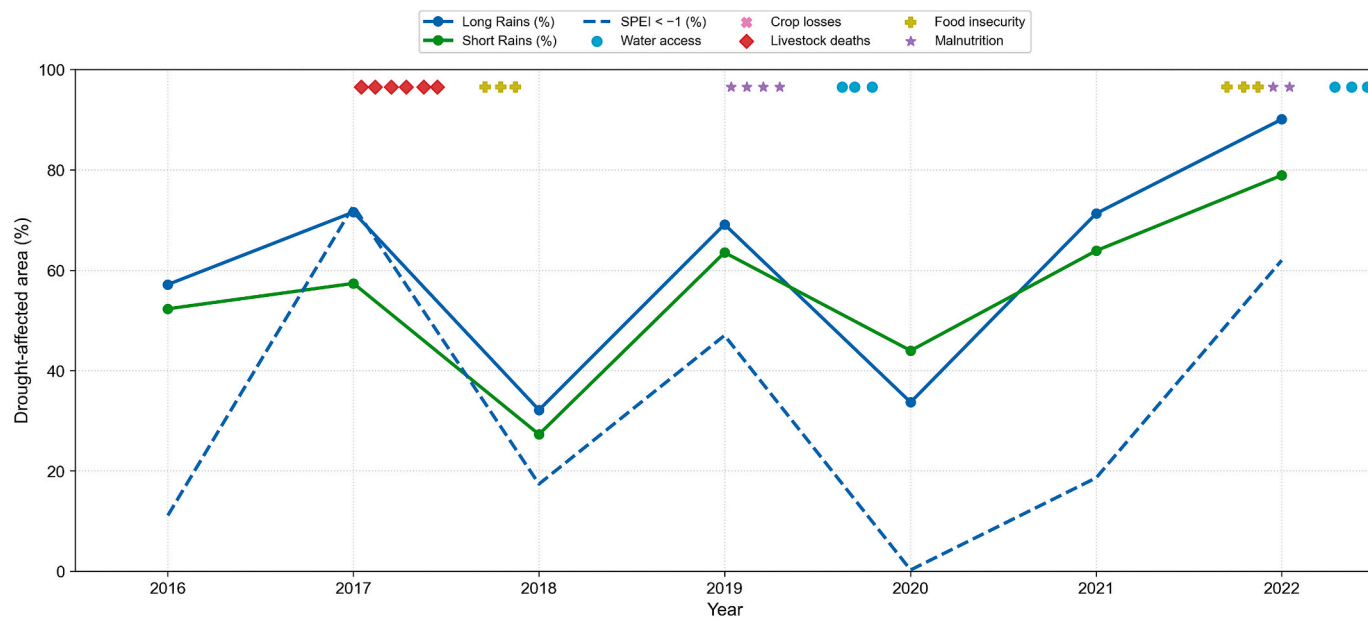


Fig. 7. Drought-affected cropland area in Kenya during 2016–2022, expressed as the percentage of pixels classified as stressed during the Long Rains (blue line) and Short Rains (green line). The dashed line shows the percentage of cropland months with SPEI < -1, indicating meteorological drought severity. Symbols above the panel mark drought impacts reported by NDMA. (For interpretation of the references to colour in this figure legend, the reader is referred to the web version of this article.)

the crop condition maps, as maize coverage in Kenya is expansive and produced by over 37 counties out of the total 47 counties.

Analysis of maize yields from 2017 to 2021 reveals intensifying drought impacts over time, with distinct patterns between the bimodal

rainfall seasons (Fig. 10). In 2018, the long rains experienced relatively mild drought, reflected in the highest yield of 1.80 tons/ha. This agrees with the crop condition mapping outcomes, indicating minimal drought impact during 2018. Conversely, years like 2021, which experienced an

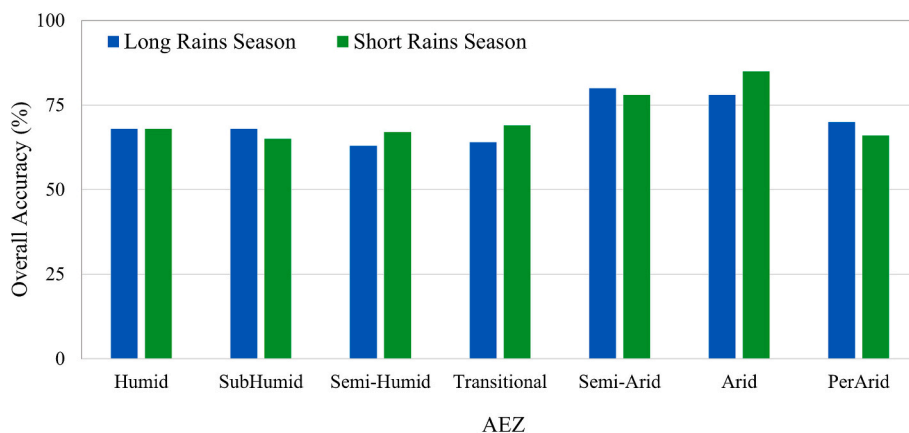


Fig. 8. Overall accuracy (in percentage) of drought impact assessment models across different AEZ in Kenya, comparing performance during the long rains season (blue) and short rains season (green). (For interpretation of the references to colour in this figure legend, the reader is referred to the web version of this article.)

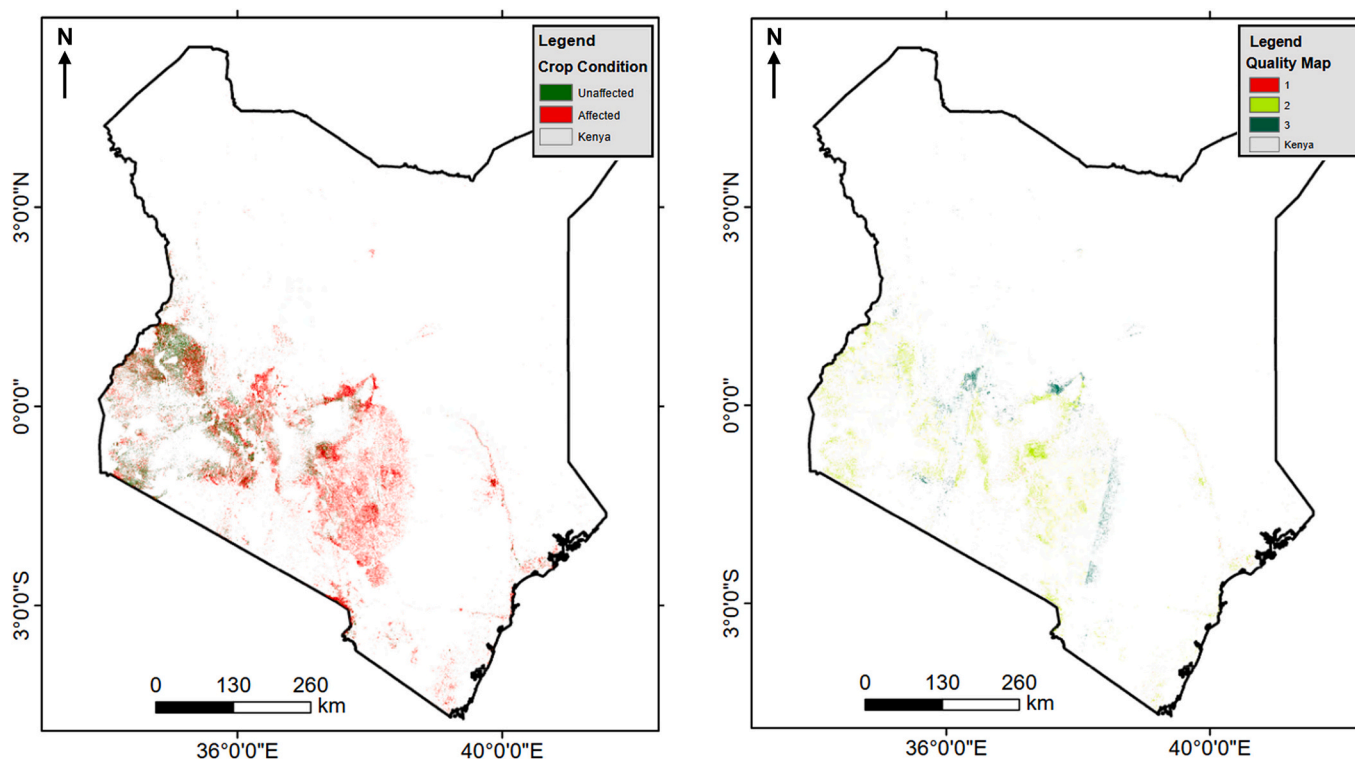


Fig. 9. Crop condition map (left) showing unaffected (green) and affected (red) areas, alongside its complementary quality map (right) for the 2019 long rains season in Kenya. The quality map categorizes data reliability from 1 (lowest) to 3 (highest). (For interpretation of the references to colour in this figure legend, the reader is referred to the web version of this article.)

intensification of drought stress as indicated by the crop condition mapping, recorded a significant decline in yields and around 0.42 tons decrease from 2018. The Z-score for 2021 aligns with the increasing drought-affected cropland coverage observed in the results. The short rains season presents a sharper decline in yields over the same period, with an average yield of 0.97 tons/ha. The Z-score of -1.10 in 2021 emphasizes the worsening drought conditions indicated in the crop condition maps.

These trends reveal critical insights into agricultural planning and food security, highlighting the broader trend of increasing drought intensity and its effects on maize yields in both seasons. First, drought intensity has clearly escalated over the study period, with 2021 showing the most severe impacts across both seasons. Second, the variance in average yields between the long and short rains seasons underscores the

differential impact of drought timing and severity. While the long rains season tends to yield higher productivity, it also shows a decline regarding prolonged drought periods. The short rains season demonstrates higher climatic vulnerability than the long rains, likely due to its critical timing in crop development and greater sensitivity to rainfall variability. Third, differential effects across AEZs suggest that drought impacts are not uniform, necessitating zone-specific adaptation strategies. The strong correspondence between remote sensing-derived crop conditions, NDMA reports, and yield data confirms that satellite-based monitoring can provide timely early warning information to support drought preparedness and response planning in rainfed agricultural systems.

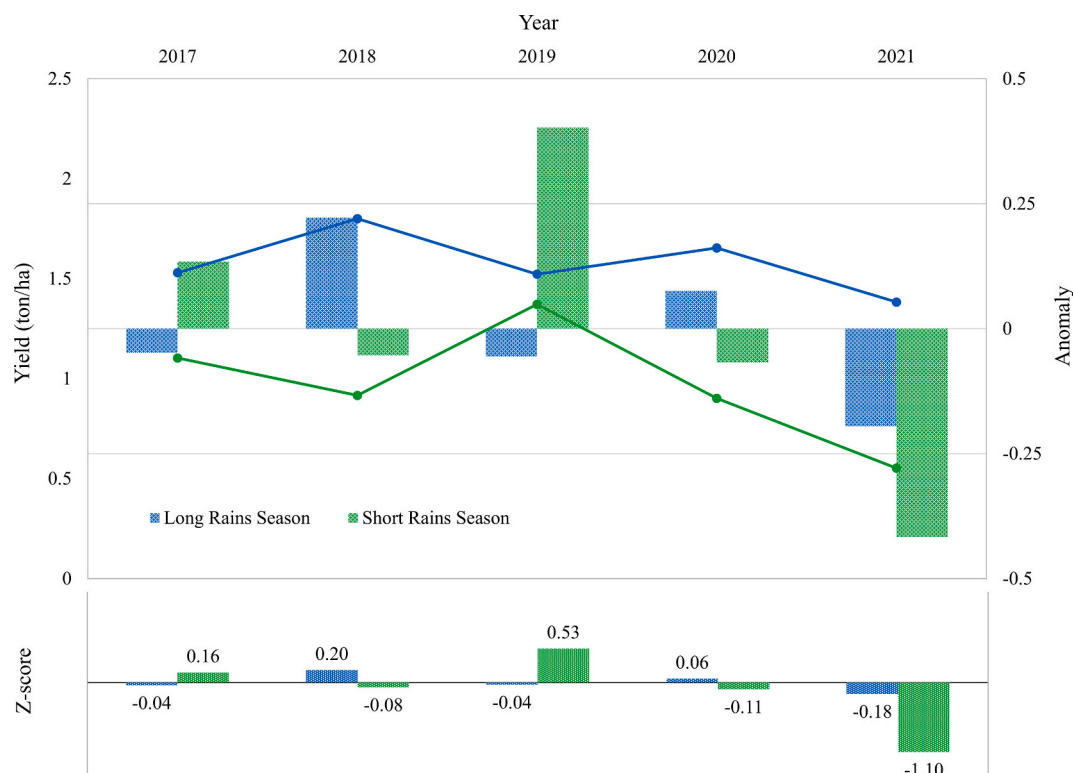


Fig. 10. Trends in maize yield productivity and drought-related anomalies (top) and Z-scores (bottom) for long (blue) and short (green) rains seasons from 2017 to 2021 of Kenya. The upper panel illustrates annual yields (lines) and their deviation from the mean (bars), while the lower panel provides a standardized measure (Z-score) of yield variation. (For interpretation of the references to colour in this figure legend, the reader is referred to the web version of this article.)

6.2. Limitations and outlook

The fluctuations in crop conditions and yields can be due to factors unrelated to drought, such as variations in farming practices, including irrigation methods not captured in statistical data, and the use of fertilizers. Additionally, changes in crop conditions can be influenced by other variables like plant diseases. Furthermore, uncertainties in cropland masks can also impact the crop condition output. Misclassified pixels (i.e., a road pixel wrongly classified as cropland) cause misinformation in training the classifier. Another significant challenge is the inherent variability in agricultural land cover, which can undergo substantial changes within short periods. Indeed, VIs of a non-cropland pixel do not provide an actual time series of a crop growing stages. Although filtering of the time series was applied, still some non-representative VIs time series may affect model training; finally, influencing the mapping accuracy.

The limitations of crop condition mapping can be categorized into two main aspects limitations caused by data availability, such as cloud free Sentinel-2 images and cropland maps, and varying on-site conditions, such as other biotic and abiotic stressors. Due to the characteristics of Sentinel-2 images, such as temporal coverage and weather conditions in the study area, the availability of Sentinel-2 images can vary. The lack of clear sky observations can cause missing values in time series. Although monthly mosaics have significantly improved the data gaps, due to consecutive cloudy days there are still missing values over some cropland pixels. While remote sensing-based methods can identify changes indicative of drought, distinguishing these from other causes of variability in crop conditions remains a complex task, often leading to uncertainties in accurately estimating the impact and timing of droughts. Specifically, The Fall Armyworm, first observed in 2016, has threatened maize crops across the country, causing substantial yield losses and economic impacts (De Groote et al., 2020). Simultaneously, Kenya experienced its worst desert locust invasion in 70 years, starting

in December 2019 (Wang et al., 2021). This invasion, which spread to 28 counties, devastated crops and vegetation, exacerbating food security concerns. This complexity underscores the need for a well-established approach in interpreting remote sensing outcomes, considering the multitude of factors that can affect agricultural land cover. These results emphasize the need for targeted interventions to enhance the resilience of crop production systems of Kenya. Strategies such as improved water management, drought-tolerant crop varieties, and adaptive agronomic practices can mitigate the adverse effects of drought and stabilize crops yields. Moreover, integrating spatially detailed crop condition monitoring with yield projections can support more effective decision-making and resource allocation in agricultural planning.

Beyond the limitation, this study demonstrates notable advancements in drought monitoring and agricultural risk assessment using high-resolution (20-m) crop condition maps at a national scale over seven years and two growing seasons. By providing detailed and field-level insights, the proposed approach addresses gaps in past studies that relied on moderate-resolution data, enabling precise identification of drought-affected areas and tailoring interventions to local needs. The comprehensive national-scale monitoring captures regional variations across AEZ of Kenya, while the seasonal analysis highlights the distinct impacts of drought during long and short rains. Additionally, the temporal trends over seven years reveal increasing drought severity, emphasizing the urgency for resilience-building measures and can serve as input to early warning and food security assessment frameworks (Barrett et al., 2020; Krishnamurthy R et al., 2022).

The proposed framework holds significant potential for operational applications beyond retrospective analysis. First, the workflow can be adapted for near real time monitoring by processing incoming Sentinel-2 observations on a rolling basis, enabling detection of emerging drought conditions within 2 to 3 weeks of image acquisition. This capability would support timely early warning and rapid response. Second, the outputs can be integrated into existing early warning systems, such as

FEWS NET and NDMA frameworks, to enhance spatial resolution and enable field level targeting of interventions. The 20 m products provide substantially more spatial detail than currently available moderate resolution products, potentially improving precision of food security assessments and resource allocation. Third, the methodology demonstrates transferability potential to other East African countries with similar bimodal rainfall patterns.

7. Conclusion

This study demonstrates the feasibility and benefits of field-scale drought monitoring across AEZ of Kenya using high-resolution Sentinel-2 observations and machine learning. By stratifying both the bimodal growing seasons and distinct agro-ecological contexts, our approach captures localized variability in drought effects. The proposed framework, driven by VIs successfully identifies drought-affected areas, showing meaningful correlation with governmental yield statistics and NDMA reports for most regions and seasons. Results from 2016 to 2022 highlight an escalation of drought severity over time, with 2018 experiencing minimal drought impacts and 2022 exhibiting extensive crop stress in both long and short rains seasons. In particular, the long rains season of 2022 saw over 90% of croplands affected by drought in some AEZ, underscoring the growing vulnerability of agriculture to climate extremes. Nevertheless, the method has inherent uncertainties arising from persistent cloud cover, other abiotic and biotic stressors, and possible land-cover misclassification, which can confound drought signals. Despite these limitations, this study provides operationally relevant, high-resolution crop condition maps that can guide drought risk management and targeted interventions at national to county scales. Future work could refine spatiotemporal coverage by incorporating radar-based or thermal infrared data, combining in-situ measurements, and further integrating metrics (e.g., soil moisture or precipitation anomalies) to differentiate drought from other causes of reduced vegetation. Additionally, coupling these maps with yield forecasting models and near-real-time monitoring systems has significant potential to improve early warning systems, ultimately enhancing resilience to ongoing and future drought hazards.

CRediT authorship contribution statement

S. Mohammad Mirmazloumi: Visualization, Validation, Resources, Methodology, Investigation, Formal analysis, Data curation, Conceptualization. **Harison Kipkulei:** Writing – review & editing, Writing – original draft. **Rose Waswa:** Writing – review & editing, Validation. **Tobias Landmann:** Writing – review & editing, Validation. **Tom Dienya:** Writing – review & editing, Validation. **Maximilian Schwarz:** Writing – review & editing. **Fabrizio Ramoino:** Writing – review & editing. **Clément Albergel:** Writing – review & editing. **Gohar Ghazaryan:** Writing – review & editing, Writing – original draft, Methodology, Funding acquisition, Data curation, Conceptualization.

Declaration of competing interest

The authors declare that they have no known competing financial interests or personal relationships that could have appeared to influence the work reported in this paper.

Acknowledgements

The work was supported by the European Space Agency within Integrated Use of Multisource Remote Sensing Data for National-Scale Agricultural Drought Monitoring in Kenya (Adm-Kenya) project under the contract 4000139450/22/I-DT.

Appendix A. Supplementary data

Supplementary data to this article can be found online at <https://doi.org/10.1016/j.ecolind.2026.114790>.

Data availability

Data will be made available on request.

References

- Anjum, S.A., et al., 2011. Morphological, physiological and biochemical responses of plants to drought stress. *Afr. J. Agric. Res.* 2026–2032. <https://doi.org/10.21921/jas.5.3.7>.
- Barrett, A.B., et al., 2020. Forecasting vegetation condition for drought early warning systems in pastoral communities in Kenya. *Remote Sens. Environ.* 248. <https://doi.org/10.1016/j.rse.2020.111886>.
- Camps-Valls, G., et al., 2025. Artificial intelligence for modeling and understanding extreme weather and climate events. *Nature Communications* 16 (1), 1919.
- CDKN Global, 2017. The Drought in Kenya, 2016–2017. Kenya. Available at <https://reliefweb.int/report/kenya/drought-kenya-2016-2017>.
- De Groote, H., et al., 2020. Spread and impact of fall armyworm (*Spodoptera frugiperda* J.E. Smith) in maize production areas of Kenya. *Agric. Ecosyst. Environ.* 292. <https://doi.org/10.1016/j.agee.2019.106804>. Available at:
- De Vos, K., et al., 2025. Predicting below-average NDVI anomalies for agricultural drought impact forecasting. *Remote Sens. Environ.* 330. <https://www.sciencedirect.com/science/article/pii/S0034425725003840>. Accessed: 31 August 2025.
- D'Ercole, R., et al., 2024. A high temporal resolution NDVI time series to monitor drought events in the horn of Africa. *Int. J. Appl. Earth Obs. Geoinf.* 135. <https://doi.org/10.1016/j.jag.2024.104264>.
- Descals, A., et al., 2025. Evaluating Sentinel-2 for monitoring drought-induced crop failure in winter cereals. *Remote Sens.* 17 (2). <https://doi.org/10.3390/rs17020340>.
- Du, L., et al., 2013. A comprehensive drought monitoring method integrating MODIS and TRMM data. *Int. J. Appl. Earth Obs. Geoinf.* 23 (1), 245–253. <https://doi.org/10.1016/j.jag.2012.09.010>.
- ESA, 2024. Sentinel-2 Products Specification Document. S2-PDGS-CS-DI-PSD. ESA. Available at <https://sentinels.copernicus.eu/documents/d/sentinel/s2-pdgs-cs-di-psd-v15-0>.
- ESA Standard Document, 2015. SENTINEL-2 User Handbook. Available at https://sentinels.copernicus.eu/documents/247904/685211/Sentinel-2_User_Handbook.
- FAO, 2015. AQUASTAT Country Profile – Kenya. Rome, Italy. Available at <https://openknowledge.fao.org/server/api/core/bitstreams/f7c0aebf-73cd-4aa5-b128-13af54b5693b/content>.
- FAO, 2023. The impact of disasters on agriculture and food security 2023., Avoiding and reducing losses through investment in resilience. FAO, Rome, Italy. <https://doi.org/10.4060/cc7900en>.
- FAO, 2024. Africa and Near East - Seasonal - 100m - WaPOR v2. Available at: <https://data.apps.fao.org/wapor/?lang=en&share=f-e6f399c5-4a74-458c-9c30-44bb99b64c61>.
- Gebremskel, G., et al., 2019. Droughts in East Africa: causes, impacts and resilience. *Int. Earth-Sci. Rev. Elsevier*, pp. 146–161. <https://doi.org/10.1016/j.earscirev.2019.04.015>.
- Ghazaryan, G., Dubovyk, O., et al., 2020a. Local-scale agricultural drought monitoring with satellite-based multi-sensor time-series. *GISci. Remote Sens.* 57 (5), 704–718. Available at: <https://doi.org/10.1080/15481603.2020.1778332>.
- Ghazaryan, G., König, S., et al., 2020b. Analysis of drought impact on croplands from global to regional scale: a remote sensing approach. *Remote Sens.* 12 (24), 1–17. <https://doi.org/10.3390/rs12244030>.
- Haile, G.G., et al., 2020. Drought: progress in broadening its understanding. In: *Wiley Interdisciplinary Reviews: Water*, 7. <https://doi.org/10.1002/WAT2.1407>.
- Hazaymeh, K., Hassan, K.Q., 2016. Remote sensing of agricultural drought monitoring: a state of art review. *AIMS Environ. Sci.* 3 (4), 604–630. <https://doi.org/10.3934/environsci.2016.4.604>.
- Huh, J.M., Muglavai, E.M., 2010. The effects of droughts on food security in Kenya. *Int. J. Climate Change: Impacts Responses* 2 (2), 61. Available at <https://search.proquest.com/openview/42bcf25231df644935220c49b5764a6d/1?pq-origsite=gscholar&cbl=5528230> (Accessed: 8 February 2025).
- IPCC. Summary for Policymakers, 2013. In *climate change 2013: The physical science basis*. In: Contribution of Working Group I to the Fifth Assessment Report of the Intergovernmental Panel on Climate Change. Cambridge.
- Joint Research Centre, 2022. Unprecedented Drought Brings Threat of Starvation to Millions in Ethiopia, Kenya, and Somalia. JRC news and updates. Available at https://joint-research-centre.ec.europa.eu/jrc-news-and-updates/unprecedented-drought-brings-threat-starvation-millions-ethiopia-kenya-and-somalia-2022-06-09_en.
- Kandji, S.T., 2006. Drought in Kenya: climatic, economic and socio-political factors. *New Standpoints* 6, 17–23. Available at: https://scholar.google.com/scholar?hl=en&as_sdt=0%2C15&q=Drought+in+Kenya%3A+Climatic%2C+economic+and+socio-political+factors&btnG. Accessed: 8 February 2025.
- Khatami, R., Mountrakis, G., Stehman, S.V., 2017. Mapping per-pixel predicted accuracy of classified remote sensing images. *Remote Sens. Environ.* 191, 156–167. Available at: <https://doi.org/10.1016/j.rse.2017.01.025>.
- Khechba, K., et al., 2024. Design and use of a stratum-based yield predictions to address challenges associated with spatial heterogeneity and sample clustering in

- agricultural fields using remote sensing data. *Sustainability* (Switzerland) 16 (21). <https://doi.org/10.3390/su16219196>.
- Khechba, K., et al., 2025. The impact of spatiotemporal variability of environmental conditions on wheat yield forecasting using remote sensing data and machine learning. *Int. J. Appl. Earth Obs. Geoinf.* 136. <https://doi.org/10.1016/j.jag.2025.104367>.
- Kowalski, K., Okujeni, A., Hostert, P., 2023. A generalized framework for drought monitoring across central European grassland gradients with Sentinel-2 time series. *Remote Sens. Environ.* 286. <https://doi.org/10.1016/j.rse.2022.113449>.
- Krishnamurthy, R., P.K., et al., 2022. Anticipating drought-related food security changes. *Nat. Sustainability* 5 (11), 956–964. <https://doi.org/10.1038/s41893-022-00962-0>.
- Lam, M.R., et al., 2023. Linking reported drought impacts with drought indices, water scarcity and aridity: the case of Kenya. *Nat. Hazards Earth Syst. Sci.* 23 (9), 2915–2936. <https://doi.org/10.5194/nhess-23-2915-2023>.
- Leng, G., Hall, J., 2019. Crop yield sensitivity of global major agricultural countries to droughts and the projected changes in the future. *Sci. Total Environ.* 654, 811–821. <https://doi.org/10.1016/j.scitotenv.2018.10.434>.
- Lesk, C., Rowhani, P., Ramankutty, N., 2016. Influence of extreme weather disasters on global crop production. *Nature* 529 (7584), 84–87. <https://doi.org/10.1038/nature16467>.
- Monteleone, B., Bonaccorso, B., Martina, M., 2020. A joint probabilistic index for objective drought identification: the case study of Haiti. *Nat. Hazards Earth Syst. Sci.* 20 (2), 471–487. <https://doi.org/10.5194/nhess-20-471-2020>.
- Muller, J.C.-Y., 2014. Adapting to climate change and addressing drought—learning from the red cross red crescent experiences in the horn of Africa. *Weather and Climate Extremes* 3, 31–36. Available at: <https://www.sciencedirect.com/science/article/pii/S2212094714000309>. Accessed: 8 February 2025.
- National Drought and Management Authority, 2019. Annual Report and Financial Statements for Financial Year Ending 30th June 2019. Available at <https://knowledgeweb.ndma.go.ke/Public/Resources/ResourceDetails.aspx?doc=4368618e-94c2-4316-b4da-a233f265bbf9>.
- National Drought and Management Authority, 2020. Annual Report and Financial Statements for Financial Year Ending 30th June 2020. Available at <https://knowledgeweb.ndma.go.ke/Public/Resources/ResourceDetails.aspx?doc=75deebba-573b-402a-8b4c-fe1a99426cca>.
- National Drought and Management Authority, 2021. Annual Report and Financial Statements for Financial Year Ending 30TH June 2021.
- National Drought and Management Authority, 2022. Annual Report and Financial Statements for Financial Year Ending 30TH June 2022. Available at <https://knowledgeweb.ndma.go.ke/Public/Resources/ResourceDetails.aspx?doc=f146d28e-bdf4-466b-bfaf-643f79a4303e>.
- Njogu, H.W., 2022. Effects of droughts on the delivery of infrastructure services in Kenya. *Nat. Res. Forum* 46 (2), 221–244. <https://doi.org/10.1111/1477-8947.12251>.
- Owringi, M.A., et al., 2011. Drought monitoring methodology based on AVHRR images and SPOT vegetation maps. *J. Water Resource Prot.* 03 (05), 325–334. Available at: <https://doi.org/10.4236/jwarp.2011.35041>.
- Park, Seonyoung, et al., 2017. Drought monitoring using high resolution soil moisture through multi-sensor satellite data fusion over the Korean peninsula. *Agric. For. Meteorol.* 237–238, 257–269. <https://doi.org/10.1016/j.agrformet.2017.02.022>.
- Rhee, J., Im, J., Carbone, G.J., 2010. Monitoring agricultural drought for arid and humid regions using multi-sensor remote sensing data. *Remote Sens. Environ.* 114 (12), 2875–2887. <https://doi.org/10.1016/j.rse.2010.07.005>.
- Rojas, O., Vrieling, A., Rembold, F., 2011. Assessing drought probability for agricultural areas in Africa with coarse resolution remote sensing imagery. *Remote Sens. Environ.* 115 (2), 343–352. <https://doi.org/10.1016/j.rse.2010.09.006>.
- Santini, M., et al., 2022. Complex drought patterns robustly explain global yield loss for major crops. *Sci. Rep.* 12 (1). <https://doi.org/10.1038/s41598-022-09611-0>.
- Schwarz, M., et al., 2020. A spatially transferable drought hazard and drought risk modeling approach based on remote sensing data. *Remote Sens.* 12 (2), 237. <https://doi.org/10.3390/rs12020237>.
- Shen, R., et al., 2019. Construction of a drought monitoring model using deep learning based on multi-source remote sensing data. *Int. J. Appl. Earth Obs. Geoinf.* 79, 48–57. <https://doi.org/10.1016/j.jag.2019.03.006>.
- Shisanya, C.A., 1990. The 1983–1984 drought in Kenya. *J. East. Afr. Res. Dev.* 20, 127–148. Available at https://scholar.google.com/scholar?hl=en&as_sdt=0%2C15&q=THE+1983+-+1984+DROUGHT+IN+KENYA.+Journal+of+Eastern+African+Research+%26+Development%2C+20%2C+127-148&btnG. Accessed: 8 February 2025.
- Szantoi, Z., et al., 2021. Quality assurance and assessment framework for large area land cover maps validation in the Copernicus high-resolution hot spot monitoring activity. *Eur. J. Remote Sens.* 54 (1), 537–556. <https://doi.org/10.1080/22797254.2021.1978001>.
- The Core Writing Team IPCC, 2015. Climate Change 2014: Synthesis Report. Contribution of Working Groups I, II and III to the Fifth Assessment Report of the Intergovernmental Panel on Climate Change. IPCC. Gian-Kasper Plattner. Available at <https://epic.awi.de/id/eprint/37530/>. Accessed: 6 June 2023.
- Tyukavina, A., et al. Tyukavina, Alexandra, Stehman, Stephen V., Foody, Giles M., Bontemps, Sophie, Komarova, J.E.N., Tsendbazar, Nandim-Erdene, 2025. Land cover and change map accuracy assessment and area estimation good practices protocol version 1.0. In: good practices for satellite derived land product validation. And product validation subgroup (WGCV/CEOS), p. 187. <https://doi.org/10.5067/doc/ceoswgcv/lpv/lc.001>.
- Van Hoolst, R., et al., 2016. FAO'S AVHRR-based agricultural stress index system (ASIS) for global drought monitoring. *Int. J. Remote Sens.* 37 (2), 418–439. Available at: <https://doi.org/10.1080/01431161.2015.1126378>.
- Vicente-Serrano, S.M., et al., 2022. Global drought trends and future projections. *Philos. Trans. R. Soc. Lond. A. Math. Phys. Eng. Sci.* 380 (2238). <https://doi.org/10.1098/rsta.2021.0285>.
- Wang, L., et al., 2021. Using long-term earth observation data to reveal the factors contributing to the early 2020 desert locust upsurge and the resulting vegetation loss. *Remote Sens.* 13 (4), 1–19. <https://doi.org/10.3390/rs13040680>.
- Zhang, Q., et al., 2022. Multisource data-based integrated drought monitoring index: model development and application. *J. Hydrol.* 615. <https://doi.org/10.1016/j.jhydrol.2022.128644>.